



**Codes And Methods Improvements
for VVER comprehensive safety assessment**

Grant Agreement Number: 945081

Start date: 01/09/2020 - Duration: 36 Months

WP4 - Task 4.3

**D4.5 – Guideline for future VVER assembly calculation
schemes**

J.-F. Vidal, E. Garcia-Cervantes (CEA), A. Willien (EDF)
Version 1 – 29/08/2023



This project has received funding from the Euratom research and training programme 2019-2020 under grant agreement No 945081.

CAMIVVER – Grant Agreement Number: 945081

Document title	Communication and dissemination strategy plan
Author(s)	J.-F. Vidal, E. Garcia-Cervantes (CEA), A. Willien (EDF)
Document type	Deliverable
Work Package	WP4
Document number	D4.5 - version 1
Issued by	CEA
Date of completion	29/08/2023
Dissemination level	Public

Summary

The H2020 CAMIVVER project aimed to develop and improve codes and methods for VVER comprehensive safety assessment.

Within Work Package 4, Task 4.3 was dedicated to actions oriented to optimize the calculation time of the lattice scheme used at the beginning of the project (close to a reference scheme) to build the NEMESI multi-parameter neutron data library generator. The objective was to meet industrial needs without significant degradation in the quality of the results and, indeed, a considerable reduction in calculation time was obtained by introducing optimized options and recent developments of the APOLLO3[®] code. For the different stages of the calculation, the gains are the following:

Geometry and boundary conditions:

- Consideration of rotational symmetries $\pi/3$ or $2\pi/3$ of the VVER assemblies: gain by a factor of 6 or 3, both on self-shielding and flux calculation

Self-shielding:

- Cell grouping: gain by a factor of 3
- Optimisation of the self-shielding steps: gain by a factor 10

Flux calculation:

- Optimized spatial mesh in MOC flux calculation: gain by a factor of 2

Depletion:

- Spaced self-shielding: gain by a factor of 2.7
- Power normalisation and coarsened depletion mesh: gain by a factor of 1.4

Some promising options have been studied to be part of a hybrid calculation scheme allowing a further reduction of the calculation time:

- Keeping the current single-level calculation for the depletion phase,
- Introducing a double-level calculation scheme for the branch calculations phase (much more time consuming than the depletion one). Computation time reduction is achieved both in the self-shielding step (using an interface-current method on a MultiCell hexagonal geometry instead of an exact collision probability method on the exact geometry) and in the flux calculation step (using energy-condensed cross sections). However, developments in APOLLO3[®] and/or ALAMOS are required to ensure the correspondence between the MultiCell and MOC geometries. The optimization of the self-shielding steps would then be of real interest in the reduction of the calculation time since the part of self-shielding would become more important compared to that one of the flux calculation.

Approval


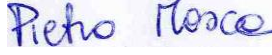

Version	First Author	WP leader	Project Coordinator
0	J.-F. Vidal (CEA) 29/08/2023	P. Mosca (CEA) 29/08/2023	D. Verrier (Framatome) 29/08/2023
	Signature 1 st author 	Signature WP leader 	Signature Coordinator 

Table of contents

Table of contents	4
List of Figures	4
List of Tables	5
1 Introduction	6
2 Assembly industrial calculation scheme initially incorporated in the NEMESI multiparameter library generator prototype	6
3 Investigations on VVER assembly industrial calculation schemes during the CAMIVVER project	9
3.1 Boundary conditions and symmetry treatment	9
3.2 Geometry and mesh for the flux calculation and sectors definition	10
3.3 Self-shielding cell grouping.....	12
3.4 Stiffener simplification for the self-shielding and flux calculations.....	14
3.5 Depletion with power normalisation.....	15
3.6 Branching calculations - self-shielding optimization	20
4 Prospects for future improvements	27
5 Conclusion	29
6 References	30

List of Figures

Figure 1. Cell discretization adopted in the reference scheme implemented in NEMESI v0 [5].	7
Figure 2. Reference scheme calculation implemented in NEMESI-0.1.	8
Figure 3. Geometry description for $\pi/3$ symmetry.....	9
Figure 4. Discrepancy between the complete assembly and the translated assembly with APOLLO3® (13AU case).	10
Figure 5. Fuel pin mesh for the reference (left) and relaxed (right) cases.	10
Figure 6. Tube-guide mesh for the reference (left) and relaxed (right) cases.....	11
Figure 7. Reference (left) and relaxed (right) control rod mesh.	11
Figure 8. K_{inf} along the burnup (left y-axis) and discrepancies between the reference and the cases with and without sectors for the flux calculations.	11
Figure 9. Delivered energy discrepancies between the reference and the relaxed mesh for the flux calculations.	12
Figure 10. Geometry for the flux calculation (A.) and individual and grouped geometries for the self-shielding calculation (respectively B. and C.)	12
Figure 11. K_{inf} along the burnup (left y-axis) and discrepancies between the reference and grouped media at the self-shielding calculation.	13
Figure 12. Delivered energy discrepancies per fuel pin between the reference and grouped media at the self-shielding calculation.	13
Figure 13. Exact (left) and simplified (right) description of the stiffener.	14
Figure 14. Reactivity difference related to the exact and diluted stiffener description and to the self-shielding of stiffener isotopes (left) and delivered energy difference between the approximate and exact stiffener description without self-shielding calculation of the stiffener's isotopes (right).	15
Figure 15. 96-step and coarsened (46-steps, bottom) depletion meshes.....	16

Figure 16. One-sixth of the assembly 439GT..... 16

Figure 17. Discrepancy on the k_{inf} between the reference calculation and case 1 (on the left) and case 2 (on the right)..... 17

Figure 18. Isotopic concentration discrepancies (^{235}U , ^{238}U , ^{239}Pu , ^{241}Pu and ^{241}Am) between the reference calculation and case 1 (left) and case 2 (right)..... 17

Figure 19. Isotopic concentration discrepancies (^{131}Xe , ^{132}Xe , ^{133}Xe , ^{134}Xe , ^{135}Xe and ^{136}Xe) between the reference calculation and case 1 (left) and case 2 (right)..... 18

Figure 20. Isotopic concentration discrepancies (^{154}Gd , ^{155}Gd , ^{156}Gd , ^{157}Gd , ^{158}Gd and ^{160}Gd) between the reference calculation and case 1 (left) and case 2 (right)..... 18

Figure 21. Normalized Gd155 and Gd157 concentrations during evolution. 18

Figure 22. 5X5 cluster geometry ($1/8^{\text{th}}$) for the self-shielding optimization of branch calculations 22

Figure 23. k_{eff} and absorption rate differences when performing systematic or spaced self-shielding (all parameters)..... 24

Figure 24. k_{eff} and absorption rate differences when performing systematic or Case 1 spaced self-shielding (rod parameter only) 25

Figure 25. k_{eff} and absorption rate differences when performing systematic or Case 2 spaced self-shielding (rod parameter only) 25

Figure 26. k_{eff} and absorption rate differences when performing systematic or Case 3 spaced self-shielding (rod parameter only) 26

Figure 27. Homogeneous hexagonal geometry for the MultiCell solver 28

List of Tables

Table 1. Comparison for the self-shielding and flux calculations between complete and $\pi/3$ symmetry case. 9

Table 2. Discrepancies on k_{inf} and time calculation for each analyzed case. 14

Table 3. Description of the analyzed cases for the flux renormalization..... 16

Table 4. Calculation time between evolution cases for the 439GT assembly..... 19

Table 5. Self-shielding burnup-up points for the different cases 22

Table 6. Calculation time for the different cases 26

Table 7. Calculation time with the TDT-CPM/TDT-MOC and MultiCell solvers..... 28

1 Introduction

The H2020 CAMIVVER project [1] aims to develop and improve codes and methods for VVER comprehensive safety assessment.

In Work Package 4 (WP4), Task 4.1 and Task 4.2 are respectively focused on the development of a multiparameter neutron data library generator prototype based on the APOLLO3[®] code [2], called NEMESI [3], and to its verification. Task 4.3 is dedicated to optimize the calculation time of the lattice scheme used in the two previous first tasks (close to a reference scheme), aiming to meet industrial needs without significant degradation in the quality of the results.

The aim of this document is to summarize the different solutions studied during the project to achieve this optimization in the calculation scheme. Perspectives for future improvements, requiring new developments in APOLLO3[®] are also proposed.

In this task, the verification and validation of APOLLO3[®] optimized calculations, performed at the assembly level, have been carried out against reference Monte Carlo continuous energy simulations with TRIPOLI-4[®][4]. The automatic tool for comparison developed as Task 4.2 contribution has not been used for this purpose here.

2 Assembly industrial calculation scheme initially incorporated in the NEMESI multiparameter library generator prototype

The description of the calculation scheme implemented at the start of the project in the NEMESI prototype multi-parameter library generator has been done in [5] and it is briefly described in this section.

The assemblies' description differs between the self-shielding and flux calculations only by the presence of sectors in the flux calculation. In both cases, there is a radial mesh in the pellet (4, 11 and 7 rings, respectively for the UOX, UGD and CR pins). The flux mesh considers a polar refinement of each cell as well as the addition of radial sectors in the moderator. The geometries for each case are displayed in Figure 1.

The reference scheme is based on a single level scheme and considers 281 energy group cross-sections (from the JEFF3.1.1 library [7] and in the 281-group SHEM energy structure [8]), the use of the Two/Three Dimension Transport (TDT) solver of APOLLO3[®] for the self-shielding and flux calculation. The self-shielding calculation is done through the Pij Collision Probability Method (TDT-CPM), whereas for the flux calculation the method of characteristics is applied (TDT-MOC). The depletion is performed with MENDEL [9], directly called by APOLLO3[®]. Figure 2 presents a diagram of the calculation scheme with its different stages.

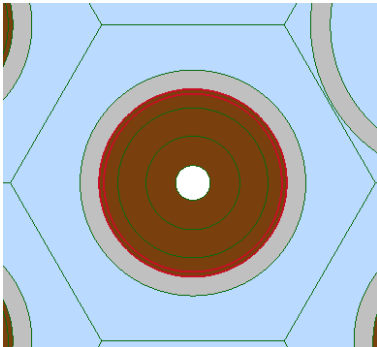
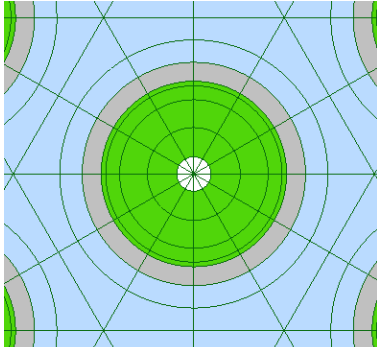
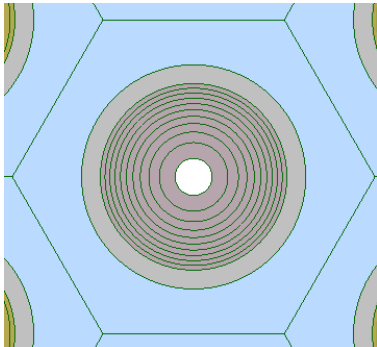
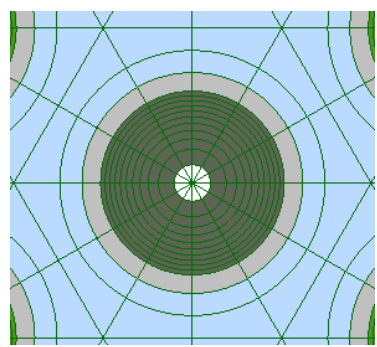
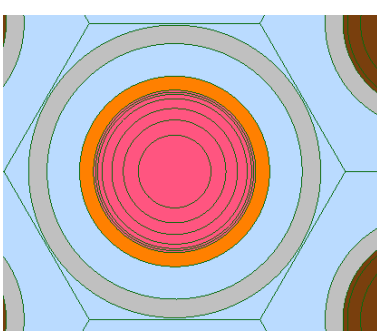
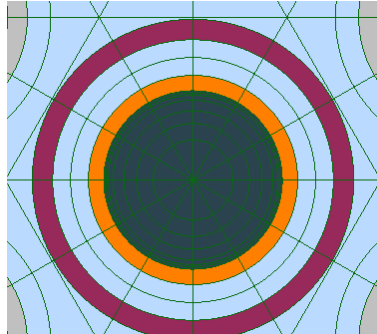
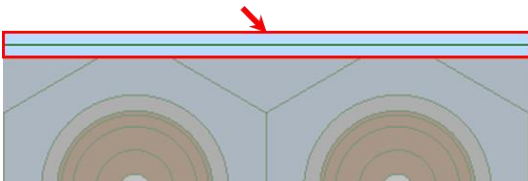
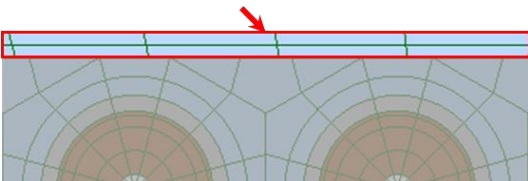
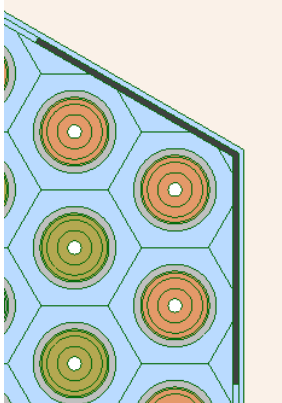
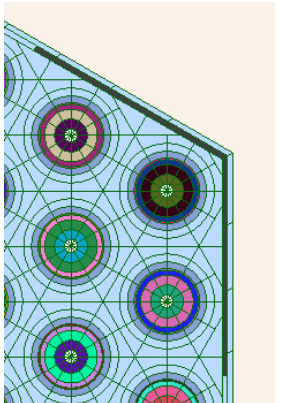
Cell type	Self-shielding geometry	Flux geometry
UOX pin		
UGD pin		
CR pin		
Water Gap		
Stiffener Plate		

Figure 1. Cell discretization adopted in the reference scheme implemented in NEMESI v0 [5].

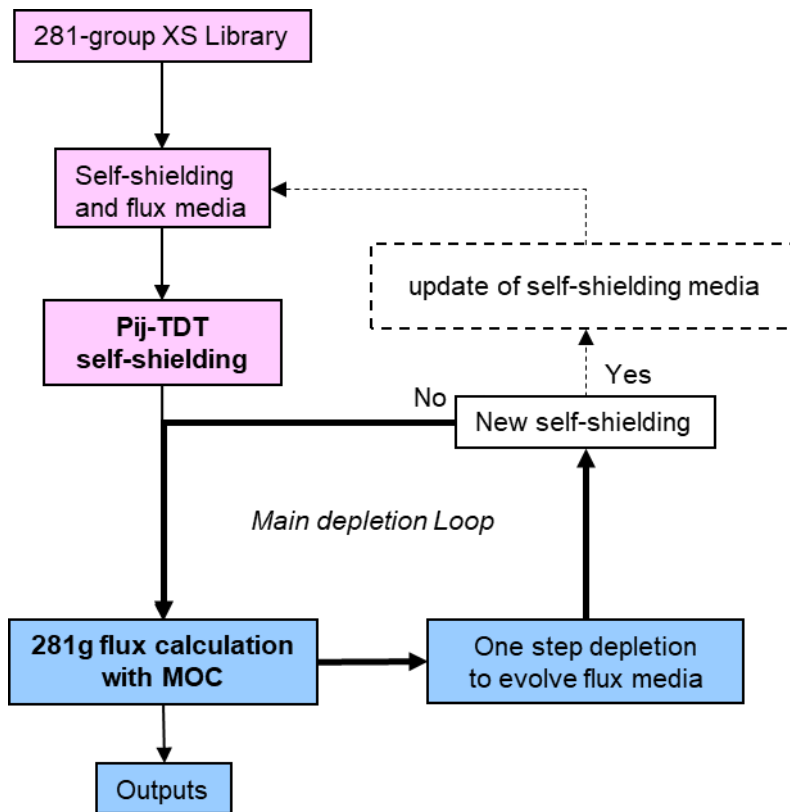


Figure 2. Reference scheme calculation implemented in NEMESI-0.1.

In this task, some considerations have been taken into account to ease the comparisons between TRIPOLI-4[®] and APOLLO3[®]. Namely, to avoid dealing with the interpolation of cross-sections at different temperatures, all temperatures (fuel, structures, and moderator) were set to 293.6 K (cold conditions)¹. As described in [6], the fuel gap is smeared with the fuel cladding. In addition, the Python interface of APOLLO3[®] is used in order to enable launching a set of calculations and to ease the output processing.

¹ The temperature conditions used in the present document differ from those in [6].

3 Investigations on VVER assembly industrial calculation schemes during the CAMIVVER project

This section provides a summary of the analysis that has been carried out for an industrial calculation scheme within the CAMIVVER project. Activities focused on verifying symmetrical conditions, coarsening sectors for the flux calculation, self-shielding with cell grouping, stiffener simplification and flux normalization along the burnup. Moreover, the analysis on the branching calculation in order to produce the multiparameter library is presented in this chapter.

3.1 Boundary conditions and symmetry treatment

Symmetry properties allow one to reduce the calculation time with deterministic tools. Among the different test cases defined for the verification, [6], there are assemblies with $\pi/3$ and $2\pi/3$ symmetries (see Figure 3). APOLLO3[®] is capable of treating both symmetries considering internal rotations and translation conditions on the external faces of the assembly. These reduced representations have been verified against the full geometries, here the results corresponding to the 13AU assembly ($\pi/3$ symmetrical case) are presented.

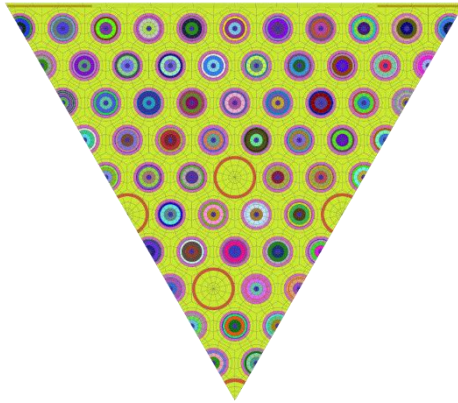


Figure 3. Geometry description for $\pi/3$ symmetry.

The discrepancies on the k_{inf} are given in Table 1, including the resulting calculation time for the self-shielding, flux calculations, the homogenization; and the Multi-Parameter Output procedures, which considers a full assembly and pin-by-pin homogenizations for a 2 energy group condensation.

Table 1. Comparison for the self-shielding and flux calculations between complete and $\pi/3$ symmetry case.

Maillage Flux	$\Delta\rho$ (pcm)	Ssh t_{calc} (s)/memory (Gb)	Flux t_{calc} (s)/memory (Gb)	$t_{homog+MPOs}$ (s)
Complete assembly	-	1805/2	720/11	922
$\pi/3$ symmetry	0	116/0.45	128/2.6	70

Since no discrepancy is found between these two cases for the k_{inf} , a local parameter such as the power distribution has also been investigated to corroborate the consistency between these two cases. Figure 4 presents the discrepancies between the two APOLLO3[®] calculations cases: they are of less than $\pm 0.4\%$. Those

discrepancies are mainly present in the edges of the assembly in which the translation boundary condition is set, and these discrepancies are considered to be acceptable.

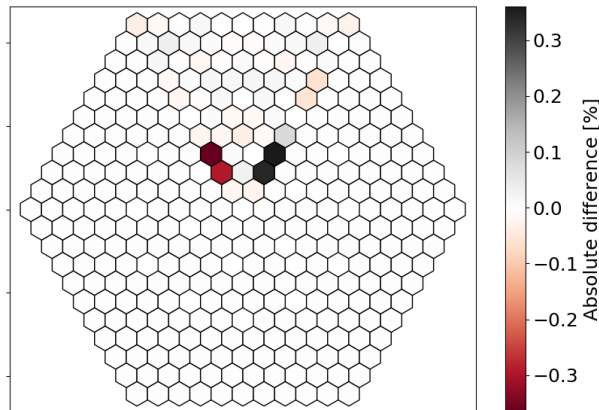


Figure 4. Discrepancy between the complete assembly and the translated assembly with APOLLO3® (13AU case).

Obviously, the gain in the computation time is considerable, so the use of the symmetrical characteristics of each assembly is strongly recommended. On the other hand, as it was shown in Table 1, the self-shielding and the flux calculations represent about 80% of the time calculation for every single step. For this reason, the investigations were focused on these two steps to decrease the calculation time in each of them.

3.2 Geometry and mesh for the flux calculation and sectors definition

A coarse spatial mesh has been proposed in order to reduce the computation time in the flux calculation. Figure 5, Figure 6 and Figure 7 present two cells with different sector definitions, one corresponding to the reference scheme (left) and a second without sectors (right) in the fuel pin, and at the center of the tube-guide and control rods cells. In fact, the coarsened mesh was based on the REL2005 scheme [10].

For the fuel pins, which are the most numerous, the number of mesh is reduced from 64 to 22 and so the computation burden required by the intersection of the characteristics with the spatial mesh.

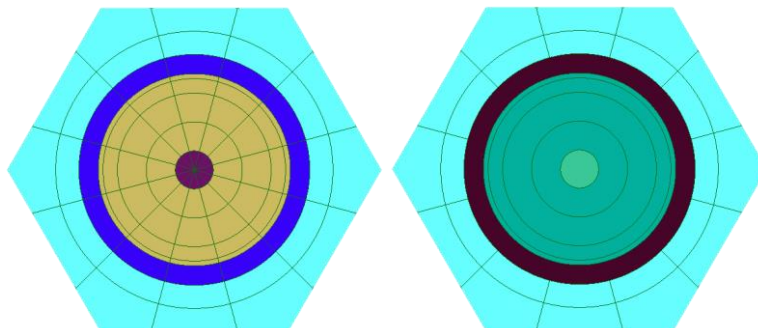


Figure 5. Fuel pin mesh for the reference (left) and relaxed (right) cases.

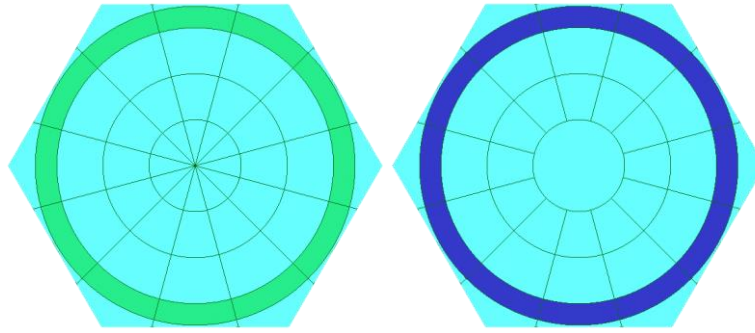


Figure 6. Tube-guide mesh for the reference (left) and relaxed (right) cases.

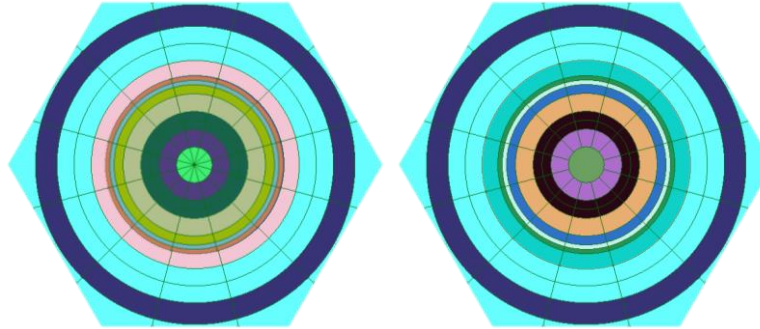


Figure 7. Reference (left) and relaxed (right) control rod mesh.

A first analysis considering these different spatial meshes is carried out for the flux calculation for the 439GT assembly. Two cases are compared with the reference scheme. For the first case, the geometry for the flux calculation has no sector. For the second one, the relaxed geometry is considered (as in Figure 5, Figure 6 and Figure 7). Depletion results for k_{inf} are compared to the reference in Figure 8.

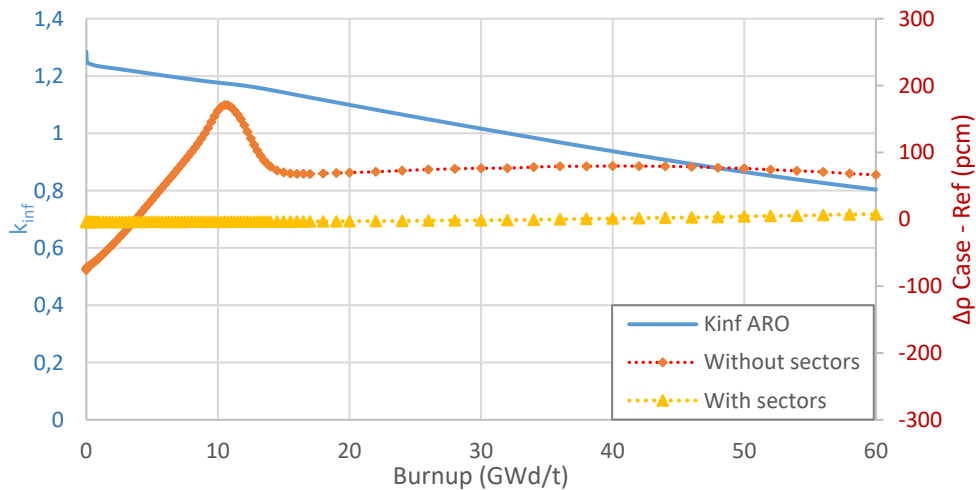


Figure 8. K_{inf} along the burnup (left y-axis) and discrepancies between the reference and the cases with and without sectors for the flux calculations.

The use of a self-shielding-like mesh exhibits large discrepancies compared to the reference, whereas the relaxed mesh presents minimal discrepancies, less than 8 pcm along the whole burnup. Local rates discrepancies, namely the delivered energy are shown in Figure 9, which exhibit minimal discrepancies, less than 0.3% in all cases. This enables to considerably reduce the calculation time for the flux (by a factor of 2) with minimal discrepancies. This relaxed mesh is recommended for future use.

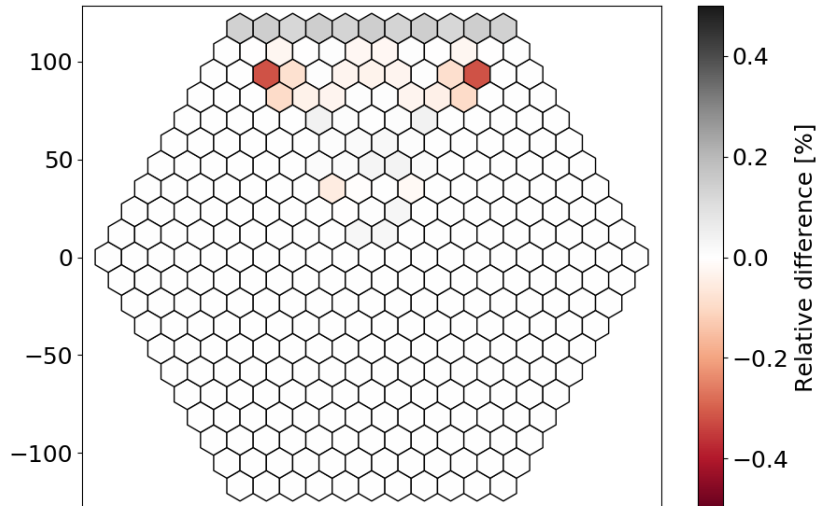


Figure 9. Delivered energy discrepancies between the reference and the relaxed mesh for the flux calculations.

3.3 Self-shielding cell grouping

Regarding the self-shielding calculation, the proposed approach is to identify a set of fuels pins that share similar surrounding physics conditions and associate them in a single group of cells. This approach is purely spatial, and five media are identified:

1. Fuel pins next to the guide-tubes;
2. Fuel pins facing angularly the guide-tubes;
3. Fuel pins whose vicinity are only fuel pins;
4. Outer fuel pins of the assembly;
5. Gadolinium absorber fuel pins.

Figure 10 shows the implemented cell grouping for the self-shielding calculation.

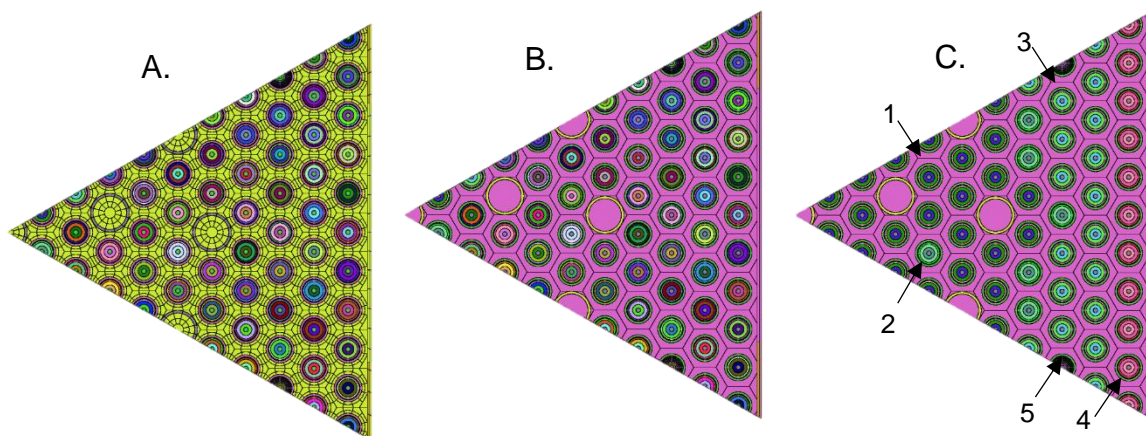


Figure 10. Geometry for the flux calculation (A.) and individual and grouped geometries for the self-shielding calculation (respectively B. and C.) .

This approach has been tested on the 439GT assembly, which presents six fuel absorber pins and 1/6th rotation symmetry. The comparison between the reference case and the proposed case has been analyzed, considering only five sets of media for all fuel cells (C.), and a relaxed spatial mesh (see section 3.2) for the flux calculation with individual media per fuel cell and ring (A.).

Figure 11 presents the k_{inf} variation with burnup up to 60 GWd/t. The discrepancies between the tested approaches and the reference are also provided on the right y-axis. The proposed approach presents reduced discrepancies, below 12 pcm, along the considered burnup. Figure 12 shows the delivered energy discrepancies between the two approaches, with minimal discrepancies below 0.01% in all cases. The asymmetric discrepancy observed near the center of the assembly is related to the presence of a gadolinium absorber pin; however, it remains very low. This approach for the self-shielding calculation is six times faster than when considering individual media per fuel cell and ring. There is a considerable gain in computation time with the use of grouped media for the self-shielding calculation.

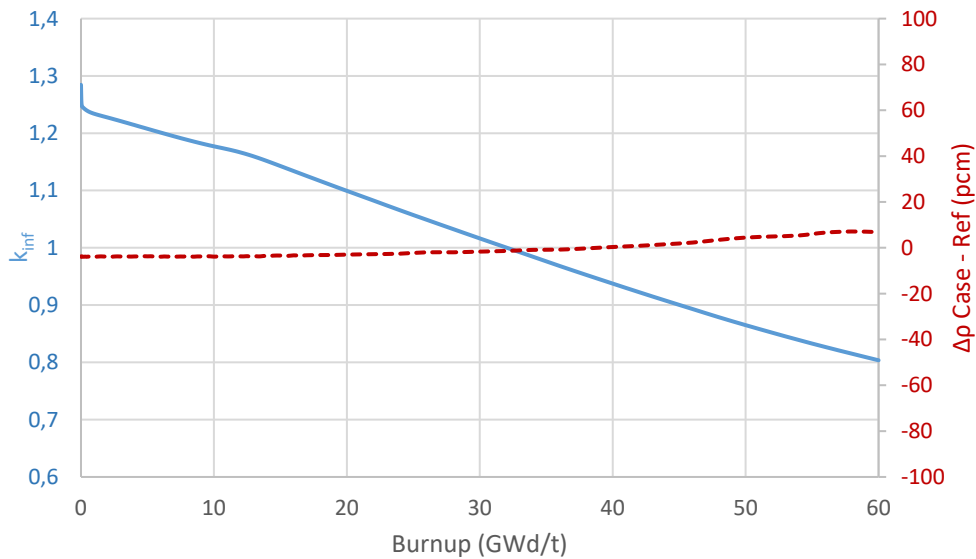


Figure 11. k_{inf} along the burnup (left y-axis) and discrepancies between the reference and grouped media at the self-shielding calculation.

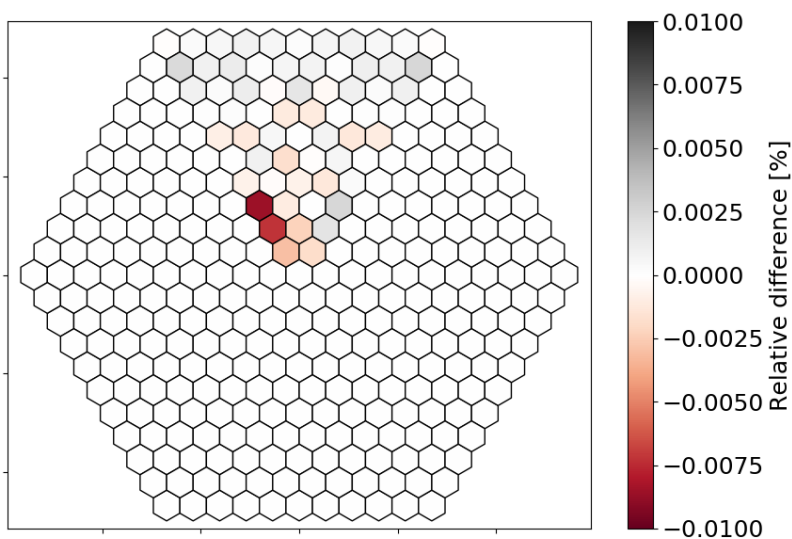


Figure 12. Delivered energy discrepancies per fuel pin between the reference and grouped media at the self-shielding calculation.

Table 2 provides the initial and maximal reactivity discrepancies together with the time for the self-shielding and flux calculations. The use of the relaxed mesh for the flux calculation and the media grouping at the self-shielding calculation provides very good agreement with the reference calculation. The global time calculation per step is reduced almost by a factor of three (2.84).

Table 2. Discrepancies on k_{inf} and time calculation for each analyzed case.

FM	RM	ISSH	GSSH	k_{inf} to/ $\Delta\rho$	max $\Delta\rho$	t in SSH	t in FLX	Total per step
✓		✓		1.27396	-	4'	5'	9'
	✓	✓		1.27386 / -6 pcm	+12 pcm (60 GWd/t)	4'	2'30"	6'30"
	✓		✓	1.27386 / -6 pcm	+11 pcm (60 GWd/t)	40s	2'30"	3'10"

FM, different mesh between the self-shielding (without sectors) and flux (with sectors) calculations.

RM, different mesh between the self-shielding (without sectors) and flux (with relaxed sectors) calculations.

ISSH, individual media per fuel cell and ring for the self-shielding calculation.

GSSH, Self-shielding media grouping.

3.4 Stiffener simplification for the self-shielding and flux calculations

In this section, the impact of the simplification of the treatment of the stiffener is analyzed in order to open the door to a multi-level calculation scheme (using for the self-shielding step the native Multicell Geometry and the approximate interface currents method available with the collision probability solver) by easing the correspondence between self-shielded and flux media. First, a spatial simplification of the stiffener for the self-shielding and flux calculations is investigated to determine whether a precise geometrical description is required, or a simplified geometry can be used (by “diluting” the stiffener, see Figure 14). Secondly, the stiffener effect on the self-shielding is analyzed simply by taking it into account and discarding it in the calculation. Figure 13 shows the exact and the simplified stiffener geometries for the 439GT assembly.

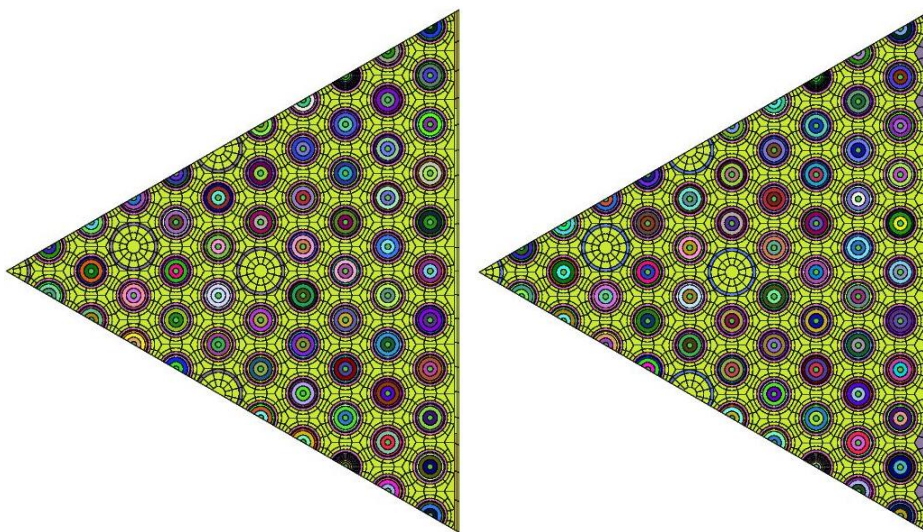


Figure 13. Exact (left) and simplified (right) description of the stiffener.

In order to assess the stiffener effect, the following comparisons have been done:

1. Exact stiffener description with and without self-shielding calculation of the stiffener's isotopes.
2. Approximate stiffener description with and without self-shielding calculation of the stiffener's isotopes.
3. Approximate and exact stiffener description with self-shielding calculation of the stiffener's isotopes.
4. Approximate and exact stiffener description without self-shielding calculation of the stiffener's isotopes.

Figure 14 presents the reactivity differences along the burnup for the selected cases and the delivered energy difference per fuel pin between the approximate and exact stiffener description without self-shielding calculation of the stiffener's isotopes. The use of a "diluted" stiffener, compared to the exact geometry, exhibits reduced discrepancies: less than 2 pcm along the burnup if the stiffener isotopes are self-shielded. The reactivity difference with and without self-shielding, for the exact stiffener also presents reduced discrepancies along the burnup, less than 10 pcm. The same discrepancy is observed for the diluted model. In other words, there is a minimal reactivity impact when the stiffener isotopes are not self-shielded and the local rates differences are negligible (less than 0.02%). To summarize, the use of a diluted stiffener without applying the self-shielding does not degrade the calculation results.

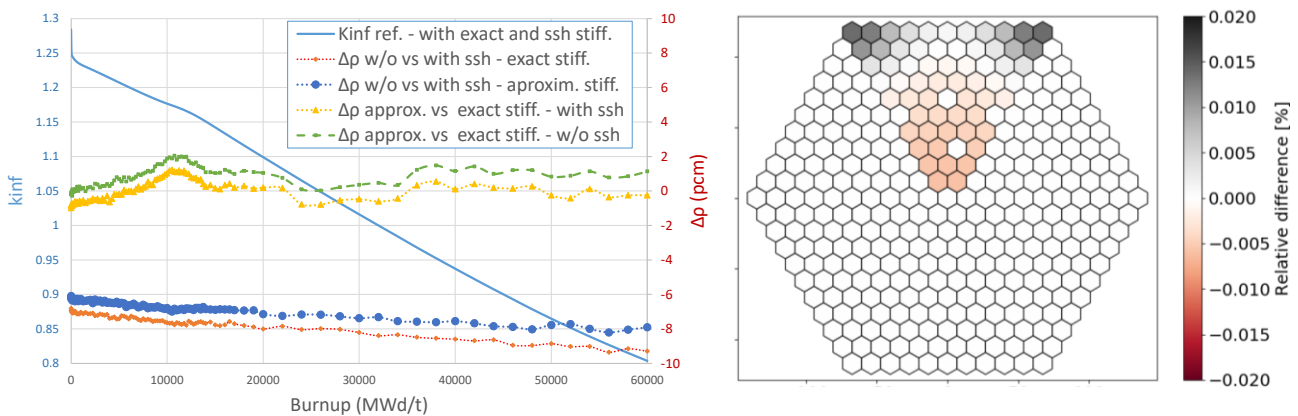


Figure 14. Reactivity difference related to the exact and diluted stiffener description and to the self-shielding of stiffener isotopes (left) and delivered energy difference between the approximate and exact stiffener description without self-shielding calculation of the stiffener's isotopes (right).

3.5 Depletion with power normalisation

Until now, the proposed approaches have focused only on flux and self-shielding static calculations. In this section, we examine a procedure to reduce the number of burnup steps through a flux renormalization procedure. Traditionally, the hypothesis for depletion calculations considers a constant flux for a fixed burnup step, through which the isotopic concentrations evolve depending on the reaction rates obtained from this flux calculation.

In this section, a flux renormalization to the assembly power between the depletion steps is proposed (as in [11]). This is done by dividing the burnup steps in sub-steps in which the flux renormalization is performed. This enables to update the flux as the concentration has evolved, without the need to perform flux or self-shielding calculations. In this way, there is a possibility to reduce the number of burnup steps.

A typical depletion mesh for this application considers 96 steps. In the current analysis, a refined depletion mesh of 159 steps is also defined to validate the 96-steps mesh. In addition, a coarsened depletion mesh of 49 steps is proposed, to be used with the renormalization procedure. Figure 15 provides the depletion steps between 0 and 60 GWd/t.

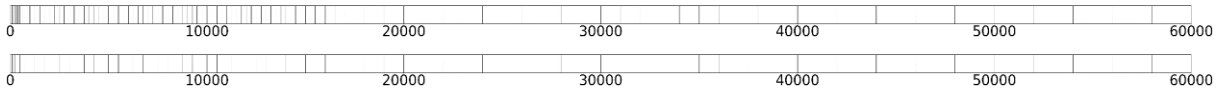


Figure 15. 96-step and coarsened (46-steps, bottom) depletion meshes.

The 439GT fuel assembly (assembly that includes Gd pins) has been selected to perform this analysis. The analyzed cases consider: 1) a 96-step depletion mesh with a self-shielding calculation at each step, 2) 96-step depletion mesh with 8 self-shielding calculations along the burnup and 3) coarse 46-steps mesh with 8 self-shielding calculations along the burnup. The first two cases do not make use of the renormalization method, while the third does. Table 3 summarizes the analyzed cases in this section.

Table 3. Description of the analyzed cases for the flux renormalization.

	Depletion mesh	Number of self-shielding calculations	Flux renormalisation
Reference	96	96	No
Case 1	96	8	No
Case 2	46	8	yes : 2 sub-steps

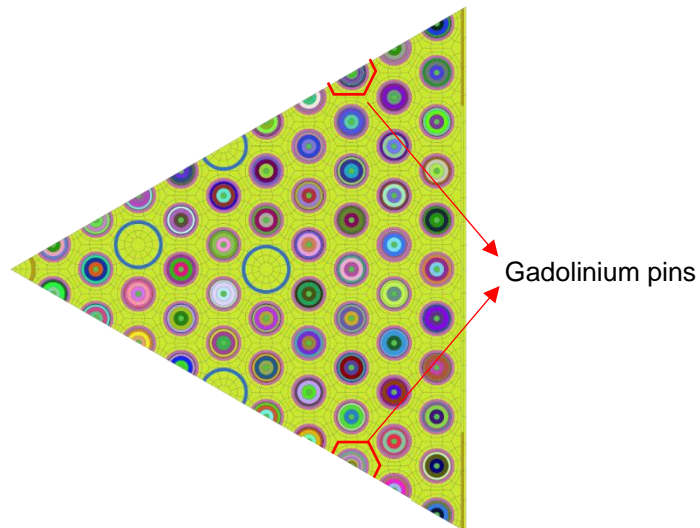


Figure 16. One-sixth of the assembly 439GT.

Figure 17 presents the discrepancies between cases 1 and 2 and the reference. These discrepancies are of the same order for both cases (about 40 pcm along the burnup). For case 2, there is a discrepancy peak of about 40 pcm at the beginning of the burnup. These discrepancies remain limited when comparing with the reference mesh.

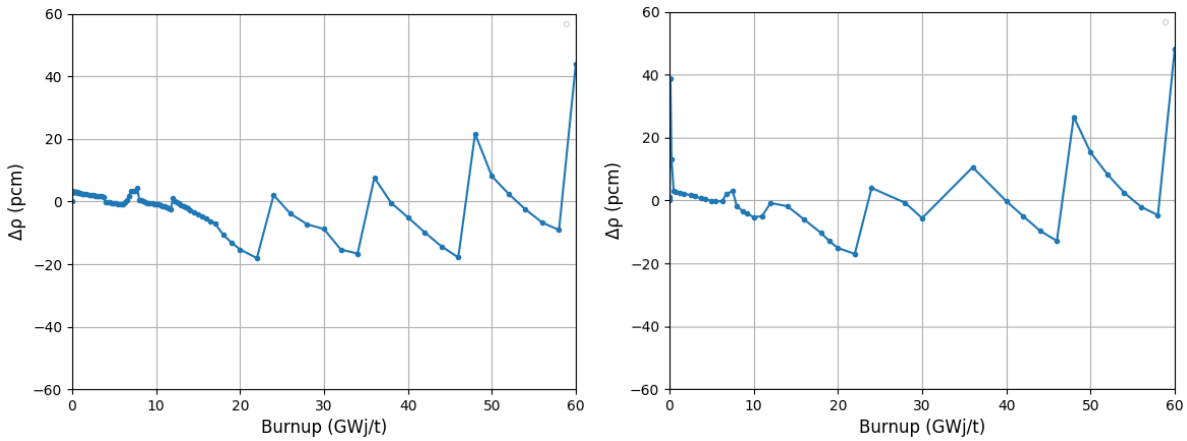


Figure 17. Discrepancy on the k_{inf} between the reference calculation and case 1 (on the left) and case 2 (on the right).

The discrepancies on the isotopic concentrations are hereafter provided to better understand the discrepancies on the k_{inf} . Figure 18 shows the isotopic concentration discrepancies between cases 1 or 2 and the reference calculation and for a set of major actinides. The case 1 discrepancies with the reference remain below $\pm 0.12\%$, while the corresponding analysis with case 2 shows larger discrepancies, just at the beginning of the burnup (about -0.6%). This explains the discrepancy peak at the beginning of the burnup seen in Figure 17.

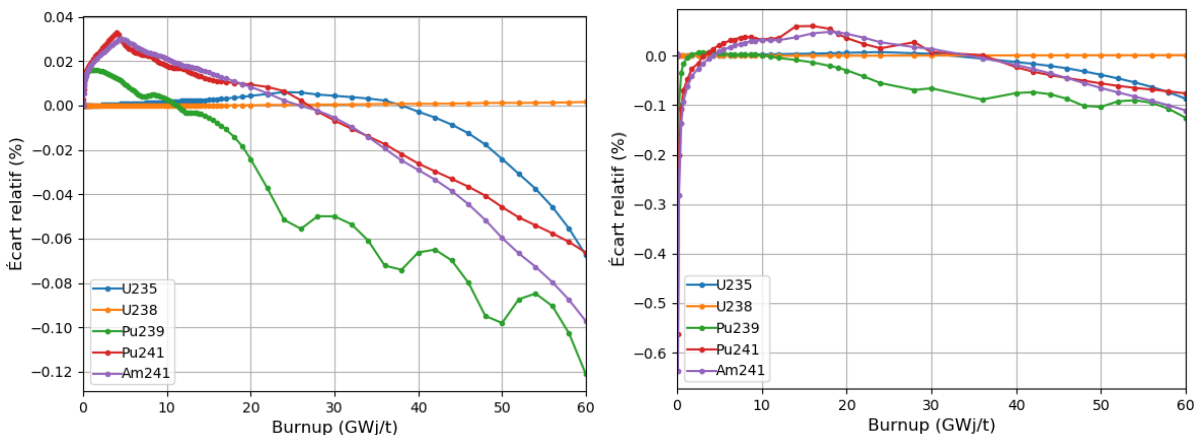


Figure 18. Isotopic concentration discrepancies (^{235}U , ^{238}U , ^{239}Pu , ^{241}Pu and ^{241}Am) between the reference calculation and case 1 (left) and case 2 (right).

Discrepancies for the Xenon isotopes are presented in Figure 19. In both cases, the discrepancies are limited below 0.1% and the larger discrepancy is seen for the ^{135}Xe isotope. Overall, these discrepancies are comparable between the case 1 and case 2.

The analysis concerning the isotopic discrepancies on the gadolinium isotopes is provided in Figure 20. In both cases, there is a discrepancy peak for the ^{155}Gd and ^{157}Gd isotopes. These error peaks are located at 14 GWd/t and 16 GWd/t respectively and correspond to 0.8% and 2% of the original isotopic concentration (see Figure 21). This shows that these discrepancy peaks do not contribute dramatically to the reactivity discrepancy, because at these points these isotopes have been mostly depleted.

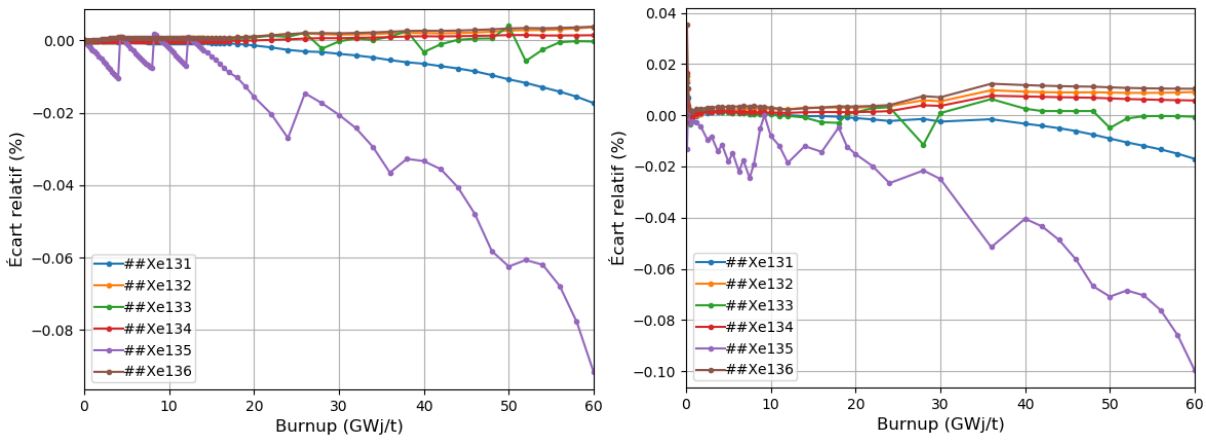


Figure 19. Isotopic concentration discrepancies (^{131}Xe , ^{132}Xe , ^{133}Xe , ^{134}Xe , ^{135}Xe and ^{136}Xe) between the reference calculation and case 1 (left) and case 2 (right).

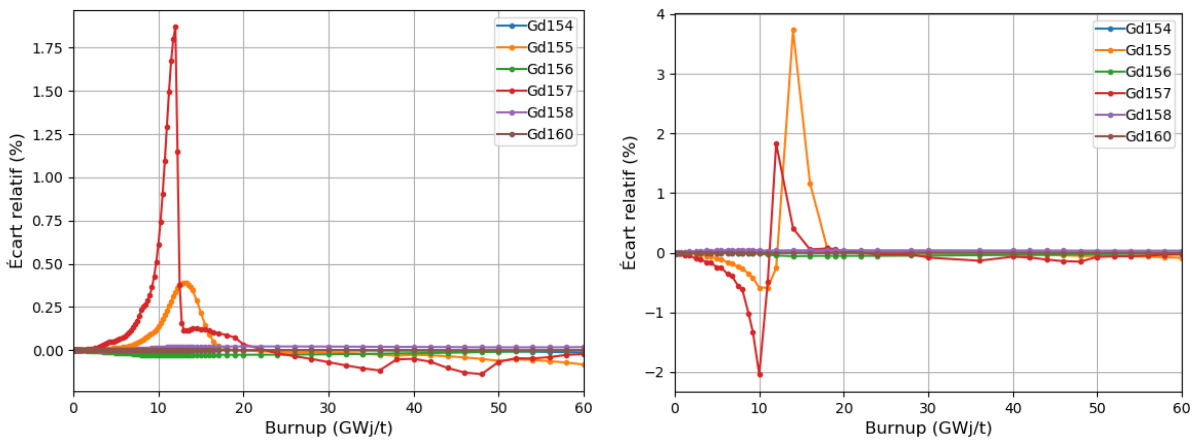


Figure 20. Isotopic concentration discrepancies (^{154}Gd , ^{155}Gd , ^{156}Gd , ^{157}Gd , ^{158}Gd and ^{160}Gd) between the reference calculation and case 1 (left) and case 2 (right).

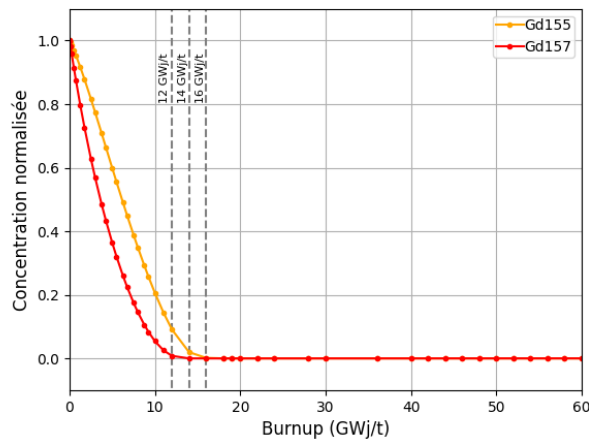


Figure 21. Normalized Gd155 and Gd157 concentrations during evolution.

Table 4. shows the computation time for each case. The reference calculation takes more than two times the time of case 1 due to the self-shielding calculations, which are done at each step. There is a gain in the time calculation when using the flux renormalization approach and coarsening the depletion mesh, with limited discrepancies compared to case 1 (5 pcm more than case 1).

Table 4. Calculation time between evolution cases for the 439GT assembly.

	Calculation time	$t/t_{\text{Case 1}}$	Max discrepancy (pcm)
Reference	3.1h	2.67	-
Case 1	1.25h	1	43
Case 2	0.9h	0.72	48

3.6 Branching calculations - self-shielding optimization

The two-step approach is used in industrial neutronic calculation schemes to allow 3D core calculations in reasonable time. This requires producing neutronic libraries containing all neutronic Quantity of Interest (QoI: cross-section, isotopic concentration, kinetic data, etc.) covering a wide range of core operating conditions (variations of power, moderator density, burn-up, media temperature, boron concentration, etc.). The crossing of these different parameters in their range of variation leads to 10000 to 20000 different calculation points that must be pre-calculated at the lattice level for the library production.

As already explained in deliverable 4.1 [12], the generation of a multi-parameter cross section library is usually divided in two phases:

- a depletion calculation at nominal (the average values of operating conditions on a cycle) or prescribed conditions, which provides isotopic concentrations for the different burn-up steps.
- branch calculations where, for each burn-up point and its corresponding isotopic compositions, the reactor operating and accidental conditions are modified one by one to produce the few-group homogenized cross sections.

The second phase takes much longer time than the first and two methods can be applied to speed it up:

- Distribute the independent calculation to parallelize the calculation effort and divide the time spent.
- Reduce the calculation time for each independent calculation by improving the industrial scheme with controlled precision.

In this study, focus is made on the second method, especially on the self-shielding step. The self-shielding step aims to produce self-shielded microscopic cross section for a set of important isotopes. These cross sections are driven by the calculation configuration and are computed before (generally fast self-shielding methods, which is the case here) or during the flux calculation (more time requiring methods), in order to correctly model spectral and spatial distribution of the neutron flux on the cross section.

In the particular case of the multi-parameter library generation, the lattice calculations are linked during the iteration on the operating conditions (also called branch calculations) and it is possible to propagate information from one calculation to the next if the new configuration is very close to the previous one, and therefore save computation time.

The only similar configurations satisfying this assumption are those with fixed temperature, material density and rod configuration, and with a slight change in isotopic concentration. This latter condition is not met for instance for ^{10}B atomic concentration: regarding the quasi-linear variation of the cross sections with this feedback parameter, few calculation points, far from each other, are used. In fact, the only feedback parameter that respects the hypothesis is the burn-up for which each burn-up point is close to its neighbors from the isotopic concentrations point of view.

In the nested loops on the different feedback parameters aiming to produce the multi-parameter library, the proposed methodology consists in using the burn-up parameter in the innermost loop and performing the self-shielding step only at certain burn-up. The Loop function used is similar to the optimized following one:

The loops encapsulating the inner burnup loop can of course be executed in parallel; only the latter must be sequential.

```

def Loop(aic):
    for fuel_temp in fuel_temp_values:
        uox31_TEM.changeTemperature(fuel_temp)
        for water_par in range(len(water_state_values)):
            water_MAT.changeMediaConcentration([H2O],[water_state_values[water_par]])
            water_TEM.changeTemperature(water_temp_values[water_par])
            xslib_MIC.run() # microlib is updated only when a temperature changes
            for boron_par in range(len(boron10_values)):
                water_MAT.changeMediaConcentration([B10],[boron10_values[boron_par]])
                water_MAT.changeMediaConcentration([B11],[boron11_values[boron_par]])
                for depStep in range(len(BudepMesh)):
                    Bu = BudepMesh[depStep]
                    print("burnup value = "+str(Bu)+" (depletion step: "+str(depStep)+)")")
                    archive_ARC.setParameterValue(Bu)
                    archive_ARC.run()
                    if REFERENCE:
                        print("    self-shielding is always performed (REFERENCE)")
                        if aic:
                            shldassm_aic_SSH.run()
                        else:
                            shldassm_SSH.run()
                    else:
                        if Bu in SshdepMesh:
                            print("    self-shielding is performed at this point")
                            if aic:
                                shldassm_aic_SSH.run()
                            else:
                                shldassm_SSH.run()
                    xslib_MAC.run() # microlib is always updated (concentrations and/or XS changes)
                    StatePointCalc(aic) # flux calculation

fuel_temp_values = [553.15, 841]
water_state_values = [2.5438E-02, 2.3709E-02]
water_temp_values = [553.15, 579.55]
boron10_values = [0., 4.7402E-06]
boron11_values = [0., 1.8961E-05]

Loop(False)

```

3.6.1 Study description

For our study, the archive-3x3cells-r.py file of the APOLLO3[®] acceptance API python test suite has been modified.

3.6.1.1 Geometry and materials

The geometry consists in a simple 5x5 cells configuration composed of 1 guide tube (with or without AIC rod inserted) surrounded by 24 UOX 3.1% pins.

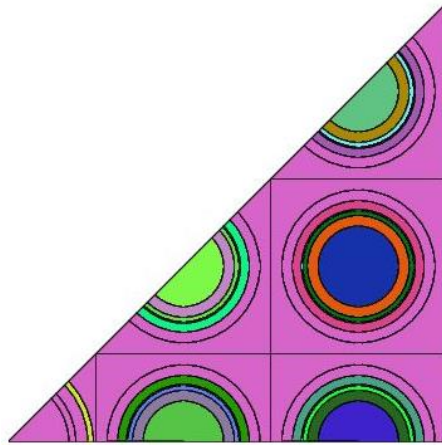


Figure 22. 5X5 cluster geometry (1/8th) for the self-shielding optimization of branch calculations

3.6.1.2 Calculations performed

The reference calculation, with self-shielding treatment performed for each calculation point, has been compared to three cases where self-shielding has been punctually computed for burnup points of the SshdepMesh list as shown in Table 5.

Table 5. Self-shielding burnup-up points for the different cases

Burnup [MW.d/t]	REFERENCE	CASE 1	CASE 2	CASE 3
0.0	X	X	X	X
9.375	X			
18.75	X			X
37.5	X			
75.	X			X
112.5	X			X
150.0	X			X
237.5	X			
325.0	X			X
412.5	X			
500.0	X			X
625.0	X			
750.0	X			
875.0	X			
1000.0	X			X
1250.0	X			
1500.0	X			
1750.0	X			
2000.0	X		X	
2250.0	X			
2500.0	X			
2750.0	X			
3000.0	X			
3250.0	X			
3500.0	X			
3750.0	X			
4000.0	X	X	X	X
4250.0	X			
4500.0	X			
4750.0	X			
5000.0	X			
5250.0	X			
5500.0	X			
5750.0	X			
6000.0	X		X	
6250.0	X			
6500.0	X			
6750.0	X			
7000.0	X			
7250.0	X			
7500.0	X			

7750.0	X			
8000.0	X	X	X	X
8250.0	X			
8500.0	X			
8750.0	X			
9000.0	X			
9250.0	X			
9500.0	X			
9750.0	X			
10000.0	X		X	
10250.0	X			
10500.0	X			
10750.0	X			
11000.0	X			
11250.0	X			
11500.0	X			
11750.0	X			
12000.0	X	X	X	X
12250.0	X			
12500.0	X			
12750.0	X			
13000.0	X			
13250.0	X			
13500.0	X			
13750.0	X			
14000.0	X		X	
14500.0	X			
15000.0	X			
15500.0	X			
16000.0	X		X	
16500.0	X			
17000.0	X			
18000.0	X		X	
19000.0	X			
20000.0	X		X	
22000.0	X			
24000.0	X	X	X	X
26000.0	X			
28000.0	X			
30000.0	X			
32000.0	X			
34000.0	X			
36000.0	X	X	X	X
38000.0	X			
40000.0	X			
42000.0	X			
44000.0	X			
46000.0	X			
48000.0	X	X	X	X
50000.0	X			
52000.0	X			
54000.0	X			
56000.0	X			
58000.0	X			
60000.0	X	X	X	X

NB: Self-shielding step for the 60000 MWd/t point has been computed for cases 1 to 3. As it is demonstrated after, it would have been more interesting to perform a self-shielding calculation at a previous burnup step to reduce the global error.

Case 1 was a first guess for testing the proposed method. The second and third cases aim to challenge case 1 elaboration for respectively medium and low burnup.

3.6.2 Results

3.6.2.1 Iteration over all feedback parameters

First calculation has been performed for the Loop function presented above but with reduced BudepMesh and SshdepMesh to save computation time, where:

- BudepMesh is the depletion step define in MWd/t;
- SshdepMesh is the burnup point (in MWd/t) at which one self-shielding procedure is called. *The burnup meshes used are:*

```
BudepMesh[:] = [0.0, 56.61, 114.75, 172.89, 335.07, 497.25, 1013.63, 530.0,
2295.0, 3060.0, 3825.0, 4590.0] #MWd/t

SshdepMesh[:] = [0.0,
172.89,
1013.63,
4590.0] #MWd/t
```

The results are shown in Figure 23, where k_{eff} and absorption reaction rate differences between the reference and the test are presented and contained within [+10; -30] pcm. We can also observe that, at first order, the error distribution does not depend on the fuel temperature nor on that of the moderator.

For burnup points shared between BudepMesh and SshdepMesh, an absolute difference of 0 is observed on the results, which means that the magnitude of the error between two points shared between the reference and the optimized industrial scheme can be easily controlled.

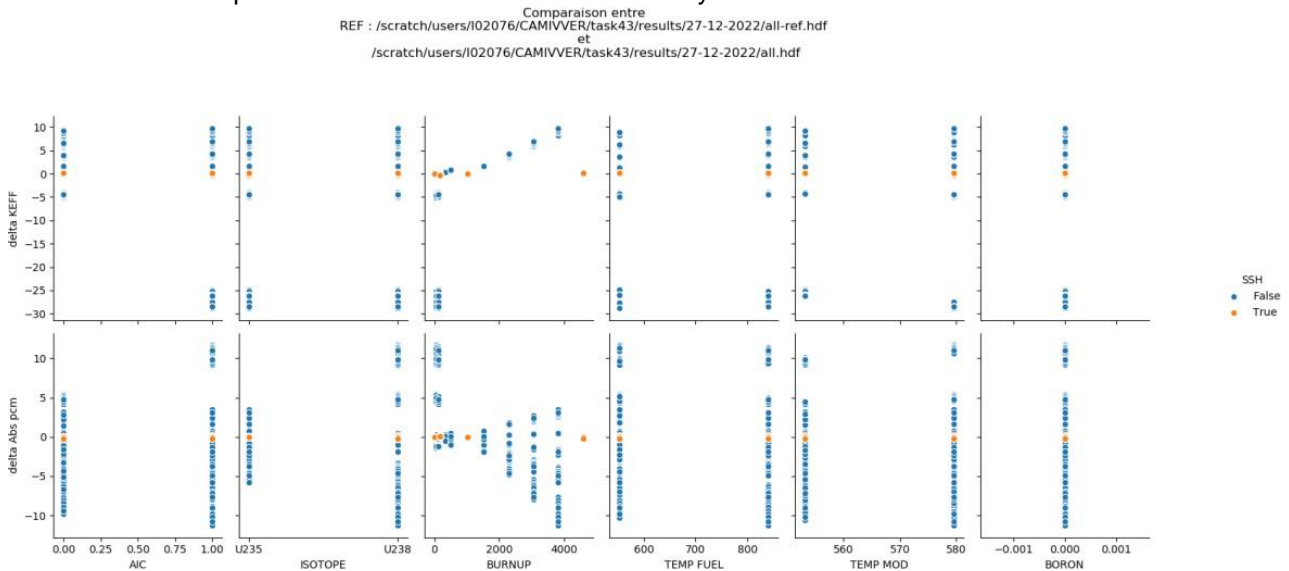


Figure 23. k_{eff} and absorption rate differences when performing systematic or spaced self-shielding (all parameters)

3.6.2.2 Iteration over burnup and rods configurations

In this part, the iteration on fuel temperature, moderator temperature and boron concentration has been disabled to optimize the computation time.

The results are shown from Figure 24 to Figure 26 (test-case 1 to 3), where k_{eff} and absorption reaction rate differences between the reference and the test are shown and contained within ± 100 pcm. For low burnup, the discrepancies are very low, and it seems not necessary to add self-shielding points. For medium and high burnup, the discrepancies are higher, and it would be a better investment to add some self-shielding points after 20000 MWd/t to improve the accuracy of the industrial scheme.

Comparison entre
 REF : /scratch/users/i02076/CAMIVVER/task43/results/27-12-2022/sensib-ref.hdf
 et
 /scratch/users/i02076/CAMIVVER/task43/results/27-12-2022/sensib-1.hdf

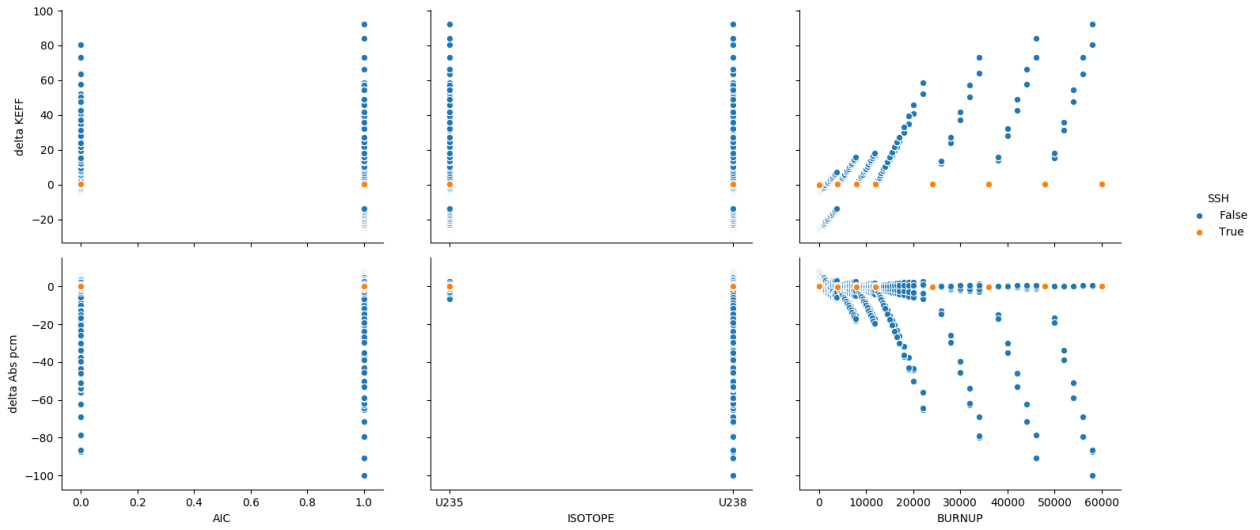


Figure 24. K_{eff} and absorption rate differences when performing systematic or Case 1 spaced self-shielding (rod parameter only)

Comparison entre
 REF : /scratch/users/i02076/CAMIVVER/task43/results/27-12-2022/sensib-ref.hdf
 et
 /scratch/users/i02076/CAMIVVER/task43/results/27-12-2022/sensib-3.hdf

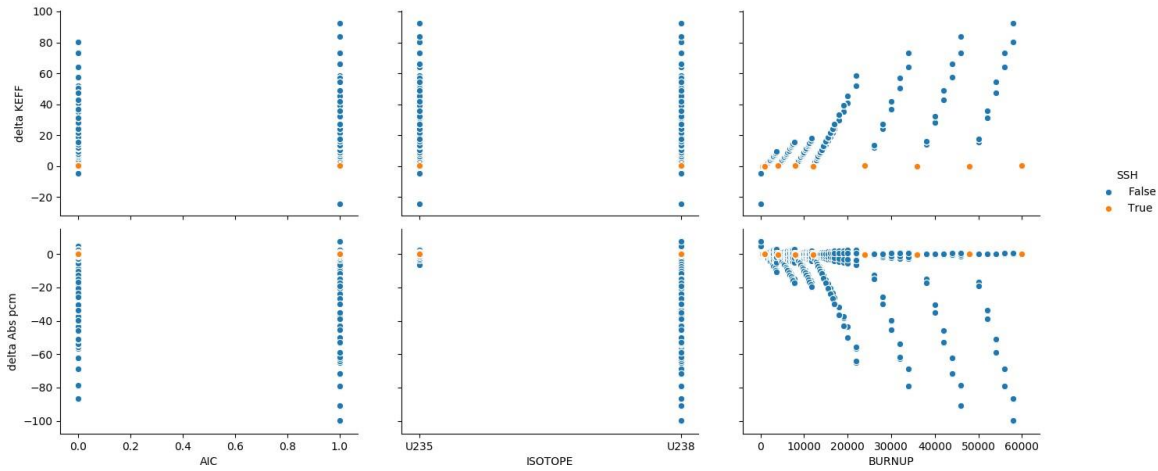


Figure 25. K_{eff} and absorption rate differences when performing systematic or Case 2 spaced self-shielding (rod parameter only)

Comparaison entre
 REF : /scratch/users/I02076/CAMIVVER/task43/results/27-12-2022/sensib-ref.hdf
 et
 /scratch/users/I02076/CAMIVVER/task43/results/27-12-2022/sensib-2.hdf

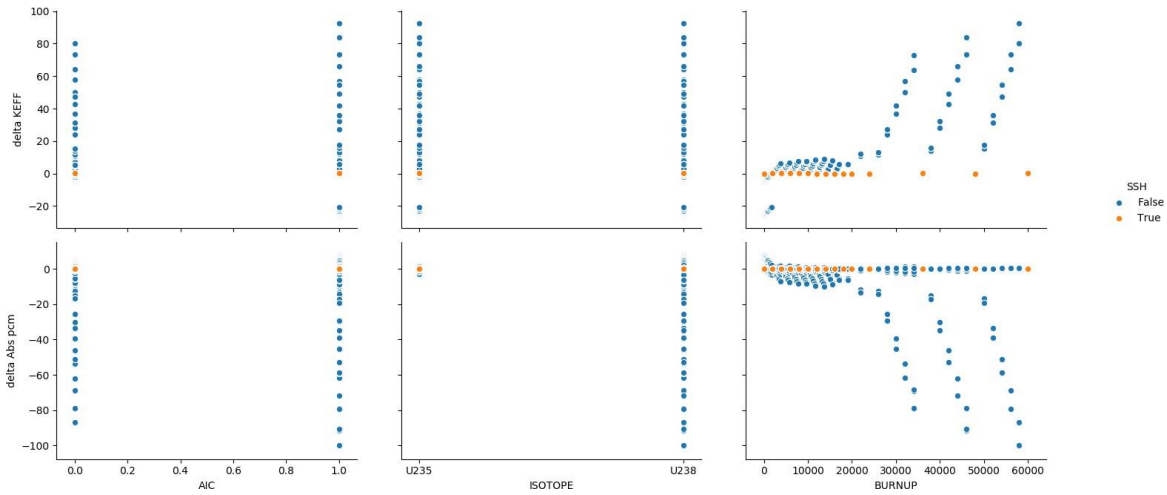


Figure 26. K_{eff} and absorption rate differences when performing systematic or Case 3 spaced self-shielding (rod parameter only)

3.6.3 Performances

The controlled precision of an industrial calculation scheme in the library generation process through limiting the number of self-shielding computation and re-use of previous self-shielded microscopic cross section has been demonstrated.

In Table 6, the computation time is presented for each case.

Table 6. Calculation time for the different cases

	REFERENCE	CASE 1	CASE 2	CASE 3
Computation Time	28'51''	26'56''	28'01''	27'35''
Delta (C/REF - 1 in %)	NA	-7 %	-3 %	-4 %

If the differences are not so large, it should be remembered that these calculations use a 281-group single-level flux calculation with TDT-MOC, which is expensive and reduces the relative share of the self-shielding step. With an industrial scheme based on a two-level scheme, the flux calculation cost would be much lower and, conversely, the self-shielding step would be longer in relative terms. Therefore, the gain of this method would be higher than that presented in the previous table.

4 Prospects for future improvements

From the optimization works presented in Chapter 3, only cell grouping have been adopted in the version of the NEMESI prototype released at the end of the CAMIVVER project (v0.2). With cell grouping, the calculation time in self-shielding is only a fraction of the calculation time in the flux calculation.

Other options allowing to further reduce the calculation time may be investigated in a next version of NEMESI, especially the use of multi-level or rather hybrid calculations scheme. If we consider the two phases of the generation of a multi-parameter cross section library, depletion and branch calculations have different needs in terms of optimization:

- the depletion calculation is performed only at nominal conditions to provide isotopic concentrations for the different burn-up steps. The number of flux calculations in this phase is very low compared to that of the branch calculations phase (about two orders of magnitude). It is therefore possible to keep a single-level scheme and take benefit of the OpenMP parallelization of the TDT-MOC solver, thus ensuring a very good precision on the concentrations, and avoiding the complexity of the reconstruction technique for treating depletion (see section 1.2 of reference [13]).
- the branch calculations must use at least a two-level calculation with a fast solver for the first level (self-shielding and 281-group flux calculation) such the MultiCell solver of APOLLO3®. The TDT-MOC flux calculation with a few ten groups at the second is fast and a large benefit can then be realized by implementing spaced self-shielding (see section 3.6).

Using the MultiCell solver is far more challenging for APOLLO3® in the VVER case than in the PWR one, in which a Cartesian geometry is used. Currently, the hexagonal MultiCell solver can only treat regular hexagonal cells, yet taking advantage of cell grouping. However, the presence of the water gaps or stiffeners at the assembly's periphery in the VVER case, make the geometry irregular and complicates the use of such a solver. Without a new development, geometrical smearing must be done in an additional ring of hexagons. We showed that it can be done with the TDT-MOC calculation without significant loss of precision.

On the other hand, the MultiCell solver currently uses native geometries while in the hexagonal case the exact geometry for the TDT-MOC solver can only be an unstructured geometry produced by an external tool as ALAMOS [14]. When using external geometries, a user-provided correspondence coming from an external tool must be entered. One possibility could be to generate the native-like geometries with the same external tool (ALAMOS for example) and to construct the association between the different geometries involved in the calculation using: a first one with a native-like description of the assembly without stiffener (see Figure 27), a second one with an unstructured description with stiffener without sectors and with the same media grouping as in the native one. Finally, a third one with an unstructured description with stiffener, sectors and individual media per pin and sectors. The additional second geometry is used as pivot in order to allow in APOLLO3® the exchange of the self-shielded cross-sections and depletion concentrations that belong on different spatial support (the former on a native-like geometry without stiffeners and the latter on the real geometry with stiffeners and sectors). There is a foreseen development in order to provide the capability in the ALAMOS to export native-like geometry recognized by the APOLLO3® code.

Preliminary tests, already reported in [13], have shown the interest of performing self-shielding calculations with the MultiCell solver considering the 30AV5 assembly. A 12th ring of homogeneous hexagonal cells has been modelled and stiffeners and water diluted consistently in both type of external cell, taking into account the cut of external fuel cells. Cells grouping for both self-shielding and flux calculations are defined regarding the cells position, as shown in Figure 27.

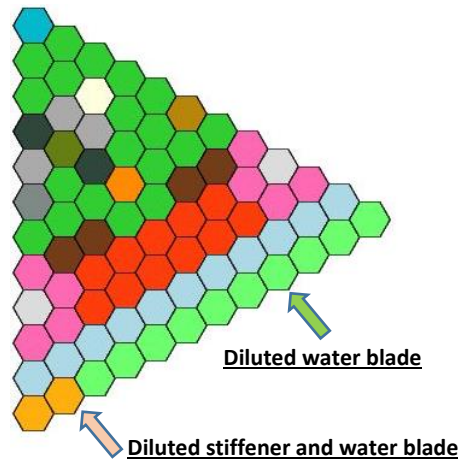


Figure 27. Homogeneous hexagonal geometry for the MultiCell solver

In Table 7 the calculation time for self-shielding calculations with different solvers is shown. The difference between the refined and coarse geometries lays in the presence or not, respectively, of radial sectors in the pin discretization. As radial sectors are necessary to capture circumferential and flux gradients between the discretized fuel pins, a coarser mesh should perform worse than a more refined representation.

As expected, the MultiCell solver provides good agreement with the reference calculation, with reduced time calculation when cell grouping is used. There is a gain factor of 25x with the MultiCell solver and reduced deviations from the reference calculation.

A single level calculation using MultiCell self-shielding and TDT-MOC flux calculation would take about 100 seconds. De facto, a multi-level calculation scheme would be of undeniable interest regarding the time of MultiCell flux calculation.

Table 7. Calculation time with the TDT-CPM/TDT-MOC and MultiCell solvers.

Calculation Time	TDT-CPM + TDT-MOC refined mesh	TDT-CPM + TDT-MOC mesh without sectors	MultiCell
$k_{inf}(t_0)$	1.07215 (ref.)	1.06822 (-343 pcm)	1.07306 (+79 pcm) (+ 57 pcm w/o groupments)
Self-shielding solver	TDT-CPM	TDT-CPM	Multicell
Time in self-shield.	911 s (4 threads)	106s (4 threads)	33s (w/o grpts: 35')
Flux Solver	TDT-MOC	TDT-MOC	Multicell
Time in flux calc.	66 s (4 threads)	23s (4 threads)	7s (w/o grpts: 14')
Total	16' 20s	2' 09s	40s (w/o grpts: ~50')

5 Conclusion

Regarding the performances of the single-level lattice calculation scheme initially defined in the NEMESI multi-parameter neutron data library generator of the CAMIVVER project, the work carried out in task 4.3 of Work Package 4 has led to a considerable reduction in calculation time by introducing optimized options and recent developments of the APOLLO3[®] code. For the different stages of the calculation, the gains are the following:

Geometry and boundary conditions:

- Consideration of rotational symmetries $\pi/3$ or $2\pi/3$ of the VVER assemblies: gain by a factor of 6 or 3, both on self-shielding and flux calculation

Self-shielding:

- Cell grouping: gain by a factor of 3
- Optimisation of the self-shielding steps: gain by a factor 10

Flux calculation:

- Optimized spatial mesh in MOC flux calculation: gain by a factor of 2

Depletion:

- Spaced self-shielding: gain by a factor of 2.7 (possibly less if greater accuracy is required)
- Power normalisation and coarsened depletion mesh: gain by a factor of 1.4

Some promising options have been studied in order to implement a hybrid calculation scheme:

- Keeping the current single-level calculation for the depletion phase,
- Introducing a double-level calculation scheme for the branch calculations phase (much more time consuming than the depletion one). This double-level scheme aimed at further reducing computation time, both in the self-shielding step (using an interface-current method on a MultiCell hexagonal geometry instead of an exact collision probability method on the exact geometry) and in the flux calculation step (using energy-condensed cross sections). However, developments in APOLLO3[®] and/or ALAMOS are required to ensure the correspondence between the MultiCell and MOC geometries. The optimization of the self-shielding steps would then be of real interest in the reduction of the calculation time since the computing time of self-shielding would become more important compared to that of the flux calculation.

6 References

- [1] CAMIVVER, "Grant Agreement number: 945081," CAMIVVER, NFRP-2019-2020.
- [2] P. Mosca et al., "APOLLO3®: Overview of the new code capabilities for reactor physics analysis", Proceedings of the International Conference on Mathematics and Computational Methods Applied to Nuclear Science and Engineering Mathematical, M&C2023, Niagara Falls, Canada, August 13-17, 2023
- [3] A. Brighenti et al., "Development of a multi-parameter library generator prototype for VVER and PWR applications based on APOLLO3®, Proceedings of the International Conference on Mathematics and Computational Methods Applied to Nuclear Science and Engineering Mathematical, M&C2023, Niagara Falls, Canada, August 13-17, 2023
- [4] E. Brun, et al. "Tripoli-4®, CEA, EDF and AREVA reference Monte Carlo code". *Annals of Nuclear Energy* 82, 151-160, 2015
- [5] A. Brighenti, L. Graziano, B. Vezzoni, "CAMIVVER - P4 - Task 4.1 - MS2 - First version of prototype based on APOLLO3®", 31/07/2022
- [6] A. Willien, B. Vezzoni, "CAMIVVER - WP4 - Task 4.2 - D4.3 Version 1 - Definitions of tests cases for the verification phases of the multi-parametric library generator", 11/02/2021
- [7] A. Santamarina et al., «JEFF3.1.1 Nuclear Data Library - Validation results from JEFF2.2 to JEFF3.1.1,» *JEFF Report 22, OECD 2009 NEA No 6807*, 2009
- [8] N. Hfaiedh and A. Santamarina (2005). "Determination of the Optimized SHEM Mesh for Neutron Transport Calculation". M&C 2005 - International Conference on Mathematics & Computational Methods Applied to Nuclear Science & Engineering, Avignon, France
- [9] S. Lahaye, et al., « Implementation of a CRAM solver in MENDEL Depletion Code System», Proceedings of the International Conference on Mathematics and Computational Methods Applied to Nuclear Science and Engineering Mathematical, Apr 2017, Jeju, South Korea, 2017
- [10] J.F. Vidal et al., "New modelling of LWR assemblies using the APOLLO2 code package", Proceedings of the Joint International Topical Meeting on Mathematics & Computation and Supercomputing in Nuclear Applications (M&C + SNA 2007), Monterey, California, April 15-19, 2007
- [11] Isotalo et al. (2016). Flux renormalization in constant power burnup calculations. *Annals of Nuclear Energy*. Volume 96, Pages 148-157, <https://doi.org/10.1016/j.anucene.2016.05.031>
- [12] A. Previti, D. Raynaud, A. Brighenti, B. Vezzoni, L. Graziano (Framatome), P. Mosca, I. Zmijarevic, J.-F. Vidal, S. Santandrea, D. Tomatis, E. Garcia-Cervantes (CEA), Y. Pipeau, A. Willien, N. Schwartz (EDF), CAMIVVER D4.1 version 1 - Representative use cases and specification requirements for the prototype multi-parametric libraries generator
- [13] E. Garcia-Cervantes, J.-F. Vidal, "CAMIVVER - WP4 - Task 4.3 - MS3 - First version of an industrial VVER scheme to be integrated in the development of the prototype"
- [14] D. Tomatis et al. (2022), "Overview of SERMA's Graphical User Interfaces for Lattice Transport Calculations", *Energies* 2022, 15, 1417